EFFECTIVE CROSS SECTIONS FOR CALCULATIONS OF CRITICALITY OF DISPERSED MEDIA

V.M. Shmakov and V.D. Lyutov
Russian Federal Nuclear Center - VNIITF
Institute of Technical Physics
P.O. Box 245, 456770, SNEZHINSK - Chelyabinsk Region, RUSSIA
Fax: +7-351-72-3-29-19, V.M.Shmakov@vniitf.ru

V.F. Dean
Consultant
HC 1 Box 407, Elgin, Arizona, USA 85611
VFDean@aol.com

ABSTRACT

Effective microscopic cross sections for fissile mixtures containing particles are presented. The continuous-energy effective cross sections are used in calculations of K_{eff} in which the mixture is represented as a homogeneous material. The formulas for the effective cross sections are based on materials of the mixture, volume fractions, and shapes and sizes of particles.

To provide a quantitative evaluation of the 'particle effect' and indicate the range of applicability of the new method of effective cross sections, K_{eff} is calculated for different variants of a heterogeneous medium consisting of spherical ^{239}Pu inclusions randomly and uniformly distributed in a water matrix. The size of Pu particles is from 5 μm to 1 cm. The Pu volume fraction varies from 0.0005 to 0.5, corresponding to H/Pu ratio from 2650 to 1.3.

Three types of K_{eff} are calculated and compared:

- K_{dir} - direct calculations of K_{eff} for the heterogeneous systems, in which the large number of Pu particles distributed in H_2O are explicitly described.
- K_{hom} - calculations of K_{eff} with traditional homogenization of the mixture, based on volume fractions.
- K_{ehom} - calculations of K_{eff} for homogeneous systems with the newly developed, effective cross sections of Pu, O and H.

Results show some large differences between K_{dir} and K_{hom}, indicating that the particle effect is large. Results also show good agreement between K_{dir} and K_{ehom}, especially for small particles. Use of effective cross sections allows replacing long-running calculations of radiation transport in a dispersed medium with faster calculations in a homogeneous system.

1. INTRODUCTION

One difficulty in predicting criticality of mixed plutonium-uranium oxide fuels or other fissile mixtures is the effect of the particulate nature of mixture components on K_{eff}. [1] Because of the finite size of particles of mixture components, calculations of K_{eff} using simple homogenization of cross sections based on volume fractions of components may not correctly predict criticality. When particle size is comparable to the mean free path of neutrons in the particle material, inner parts of the particle are shielded from neutrons by outer parts. The traditional method of homogenization of cross sections does not account for this shielding.

Traditional homogenization, which is based simply on volume fractions, does not lead to a significant error if the size of inclusions is much less than neutron and photon mean free path lengths. The mean free path of Pu fission neutrons is on the order of several centimeters. In this spectrum, homogenization will give good results for inclusions whose size is less than 1 cm.

However, in the presence of a moderator, for example water, a large number of neutrons are thermal and their fission cross sections are about 10^3 barns. Their mean free path lengths are $\sim 10^{-3}$ cm. For such systems, computational parameters may be approximated by parameters of homogeneous systems of the same mean composition only for inclusion sizes of $\sim 10^{-3}$ cm or smaller. For larger fragments, their internal areas will be screened from thermal neutrons by a layer of thickness $\sim 10^{-3}$ cm. However, such generalizations about sufficiently small particle size are much more difficult to make for a mixture of materials with cross-section resonances.

In all these cases the calculation of homogeneous systems can be conducted with the effective neutron data proposed here. These corrections to cross sections to produce the 'effective cross sections' automatically take into account the particle effect for neutrons of all energies. The new effective cross sections of materials of a matrix and included particles can be used in Monte-Carlo codes without making any changes to the scheme of trajectory modeling.

2. MODEL DESCRIPTION

To understand the derivation of the effective cross sections, the statistical model of a heterogeneous medium consisting of a mixture of inclusions, possibly of different sizes and compositions, and uniformly distributed throughout the volume of the homogeneous material of a matrix is explained. (Partial derivations of the effective cross sections were provided in [2, 5].) The formulas obtained for the effective microscopic cross sections, continuously dependent on energy, apply to both monodispersed and polydispersed media. (A polydispersed medium is one containing more than one type of particle.)

First, the formula is obtained for the effective macroscopic total cross section $\overline{\Sigma}$ of a mixture of matrix with inclusions of random form. The expression for $\overline{\Sigma}$ is then used to obtain the factors that multiply the usual microscopic cross sections to create the 'effective microscopic cross sections.' The conditions of the transition limit from effective cross section to cross section describing a homogeneous medium are also considered.

In this model description, independent variables of a function are written in parentheses as a subscript. However, after the first expression (1), the notation indicating the energy dependence of flux and cross sections is omitted. Note that, in the following discussion, neutron flux and cross sections of only one energy are considered. Of course, products of a reaction may be of any energy, but it is not necessary to consider them in order to obtain the effective cross sections.

2.1 DERIVATION OF THE EFFECTIVE MACROSCOPIC TOTAL CROSS SECTION

Attenuation of radiation in a medium may be described by the exponential law

$$I_Z = I_0 \exp(-\bar{\Sigma}_{(E)} Z). \tag{1}$$

I_0 is a flux of incident radiation (photons or neutrons or other fundamental particles) with energy E. I_Z is the same flux at the distance Z, and $\bar{\Sigma}_{(E)}$ is the effective total macroscopic cross section of the medium.

If a medium consists of a mixture of particles of one material in a matrix of another material, then a first approximation to the total macroscopic cross section of the medium can be found by assuming particle material is homogenized with the matrix. The macroscopic cross section is then

$$\bar{\Sigma} = (1-\alpha)\rho_m\sigma_m + \alpha\rho_a\sigma_a = \rho_m\sigma_m + \alpha(\rho_a\sigma_a - \rho_m\sigma_m) = \Sigma_m + \alpha\Delta\Sigma, \tag{2}$$

where $\Delta\Sigma = \Sigma_a - \Sigma_m$. This is the traditional method of homogenization of a mixture. Here α is the volume fraction of particles, $\Sigma_a=\rho_a\sigma_a$ is the total macroscopic cross section of the particle material, and $\Sigma_m=\rho_m\sigma_m$ is the total macroscopic cross section of the matrix material.

Now consider an elementary, monodirectional flux of radiation $I_0=1$ with energy E in a matrix that contains particles of equal size and shape. The particles are well mixed with the matrix, so that they are distributed uniformly, yet randomly. Suppose that the xy-plane is the surface of the system, and the radiation is incident perpendicular to the xy-plane. Also suppose that, with regard to their shape, the particles all have the same orientation with respect to the direction of the incoming radiation.

To calculate the attenuation of the radiation in a distance Z in the direction of the incident radiation, we divide Z into N equal parts, or layers. The thickness of each layer is L=Z/N. Make the three following assumptions:

1. The particles are distributed uniformly in each layer.
2. Particle distribution in one layer is independent of the distribution in other layers.
3. The chosen layer thickness L is small enough that there is no shielding effect. (This means that one particle does not shield another in the layer from radiation in the z direction; therefore uncollided radiation will enter no more than one particle per layer.)

Let's use the symbols V_0 for the volume of a particle, S_0 for the area of the projection of a particle on the xy-plane, and $p_{(t)}$ for the normalized thickness-density function of the particle in the z-direction.

Consider the flux incident on a larger area S of the xy-plane. In the layer volume V=SL, the particle volume is αSL and there will be $\alpha SL/V_0$ particles. The total projection of these particles on the xy-plane is $S_a=S_0\alpha SL/V_0$. Then the probability of interaction of the incident flux with a particle in the layer L is

$$q = \frac{S_a}{S} = \frac{\alpha L S_0}{V_0} = \frac{\alpha L}{\bar{t}}, \tag{3}$$

where $\bar{t} = \frac{V_0}{S_0} = \int t p_{(t)} dt$ is a mean chord or mean length of interception of the radiation in a particle. This may also be written

$$\bar{t} = \frac{\iint_{(x,y)\in S_0} t_{(x,y)} dxdy}{\iint_{(x,y)\in S_0} dxdy} = \frac{V_0}{S_0}, \tag{4}$$

thereby defining $p_{(t)}$, the normalized thickness-density function.

The expression for optical density of the medium must be considered. It is

$$\tau_{(L_1, L_2, ..., L_N)} = \Sigma_m \sum_{i=1}^{N} (L - t_i) + \Sigma_a \sum_{i=1}^{N} t_i = \Sigma_m NL + \Delta\Sigma \sum_{i=1}^{N} t_i , \tag{5}$$

with $\Delta\Sigma = \Sigma_a - \Sigma_m$, and t_i is the part of the radiation path within the particle in layer L_i. Recall that t_i will be the path length in only one particle per layer. For a particular path through layer L_i, it is possible that the radiation does not hit a particle, in which case t_i is zero. The attenuation of radiation that follows the path (5) through the medium is $\exp\left(-\tau_{(L_1, L_2, ..., L_N)}\right)$.

In the next step, we consider radiation falling on a unit area of the xy-plane. We define the density function of radiation in the layer L.

$$f_{(L)} = (1-q)\delta_{(t)} + q p_{(t)} , \tag{6}$$

where (1-q) is the probability to avoid collision with a particle in the layer L, q (3) is the probability of collision with a particle in the layer L, and $\delta(t)$ is the Dirac delta function. Due to the second assumption about independent distribution of particles in different layers, the density function for Z, which is made of the N independent layers, is a product of the $f(L_i)$'s:

$$F(L_1, L_2, ..., L_N) = \prod_{i=1}^{N} f(L_i) . \tag{7}$$

Use (5), (6) and (7) to find the average flux at Z, $\bar{I}_{(Z,\Sigma m,\Sigma a)} = \exp(-\tau_{(L_1, L_2, ..., L_N)})$. Because of the chosen form of the expression (6), the integration in each layer is performed only over the particle, from t=0 to $t=t_{max}$ of the particle thickness in the z direction.

$$\bar{I}_{(Z,\Sigma m,\Sigma a)} = \int_{L1} ... \int_{LN} I_{(\tau)} F_{(L1,...,LN)} dz_1 ... dz_N$$

$$= \int_{L1} \exp(-\Sigma_m L) \exp(-\Delta\Sigma t) \left[(1-q)\delta(t) + q p_{(t)}\right] dz \cdot \int_{L2} \exp(-\Sigma_m L) ... \cdot \int_{LN} ...$$

$$= \int_{t1} \exp(-\Sigma_m L)\left[(1-q)\delta(t) + q\exp(-\Delta\Sigma t)\, p_{(t)}\right]dt \cdot \int_{t2} \exp(-\Sigma_m L)\ldots \cdot \int_{tN} \ldots$$

$$= \exp(-\Sigma_m Z) \times \left[1 - q + q\int \exp(-\Delta\Sigma t)\, p_{(t)} dt\right]^N . \qquad (8)$$

Considering expressions (8) and (1), we can define the effective macroscopic cross section (cm^{-1})

$$\overline{\Sigma} = \Sigma_m - \frac{1}{L}\ln\left[1 - q + q\int \exp(-\Delta\Sigma t) p_{(t)} dt\right]. \qquad (9)$$

If we take into account expression (3), we can rewrite (9) as

$$\overline{\Sigma} = \Sigma_m - \frac{1}{L}\ln\left[1 - \frac{\alpha L}{\bar{t}} + \frac{\alpha L}{\bar{t}}\int \exp(-\Delta\Sigma t) p_{(t)} dt\right]. \qquad (10)$$

Analyzing expression (9) or (10), we can note the transition from effective to homogeneous cross sections in the limits of small or few inclusions. At $\alpha \to 0$ or $\Delta\Sigma \to 0$, both these expressions approach expression (2). Additionally, at a constant volume fraction α of inclusion, we observe that (10) approaches expression (2) with decrease of inclusion size ($\bar{t} \to 0$).

If the matrix contains inclusions of different sizes, shapes, and compositions, then expression (9) is generalized to become

$$\overline{\Sigma} = \Sigma_m - \sum_k \frac{1}{L_k}\ln\left[1 - q_k + q_k \int \exp(-\Delta\Sigma_k t) p_{k(t)} dt\right]. \qquad (11)$$

Here we sum on k types of particles. Each type is characterized by its α_k, L_k, $\Delta\Sigma_k$, q_k and $p_{k(t)}$. Note that q_k, $p_{k(t)}$, and choice of L_k are dependent on particle size, shape and orientation with respect to the direction of incident radiation.

2.2 EFFECTIVE MACROSCOPIC CROSS SECTIONS FOR PARTICULAR PARTICLE SHAPES

In [5] the expressions for effective macroscopic total cross sections for a matrix with inclusions in the form of spheres, discs, cubes and threads were presented. The expressions for spheres and cubes [2] are repeated here.

It should be mentioned that for spherical particles only, the effective cross sections do not depend on the direction of the incident radiation. For other particle shapes, the orientation of a particle relative to the direction of radiation must be taken into account. The orientation affects S_0 and $\bar{t}$, which affect the probability q (3) of the radiation's interaction with a particle in the layer.

It should also be noted that the parameter L is a free one and can be defined from various considerations, for example, from the condition of minimizing flux dispersion, defined by

$$D(I_{(\tau)}) = \int_{t1}\ldots\int_{tN} (I - \bar{I})^2 F_{(t1,\ldots,tN)} dt_1 \ldots dt_N = \bar{I}_{(z,2\Sigma m,2\Sigma a)} - \bar{I}^2_{(z,\Sigma m,\Sigma a)}. \qquad (12)$$

Here we give expressions for $p_{k(t)}$, q, L, and $\bar{t}$ for minimal L. By requiring this condition, we at least eliminate the possibility of shielding in the layer L and obtain relatively simple formulas.

In the case of **cubic particles** of edge h, for flux incident perpendicular to a surface of the cube, $p_{(t)}=\delta(t-h)$, $\bar{t}=h$, L=h, $q=\alpha$, and the effective macroscopic total cross section is

$$\overline{\Sigma} = \Sigma_m - \frac{1}{h}\ln\left[1-\alpha+\alpha\exp(-h\Delta\Sigma)\right]. \tag{13}$$

In the case of **spherical particles** of diameter D, $p_{(t)}=2t/D^2$, $\bar{t}=2D/3$, L=D, $q=3\alpha/2$, and the macroscopic total cross section for the mixture is

$$\overline{\Sigma} = \Sigma_m - \frac{1}{D}\ln\left[1-\frac{3\alpha}{2}\left(1-J_{(-D\Delta\Sigma)}\right)\right], \tag{14}$$

where[1] $$J_{(-D\Delta\Sigma)} = \frac{2}{(D\Delta\Sigma)^2}\left[1-(1+D\Delta\Sigma)\exp(-D\Delta\Sigma)\right].$$

2.3 EFFECTIVE MACROSCOPIC TOTAL CROSS SECTIONS FOR A MIXTURE OF PU PARTICLES IN WATER

The effective macroscopic total cross sections for mixtures of spherical Pu^{239} particles in water are shown in Figure 1 for particle diameters D = [0, 50, 100, 200, 500] μm at a ^{239}Pu volume fraction of $\alpha = 0.02$.

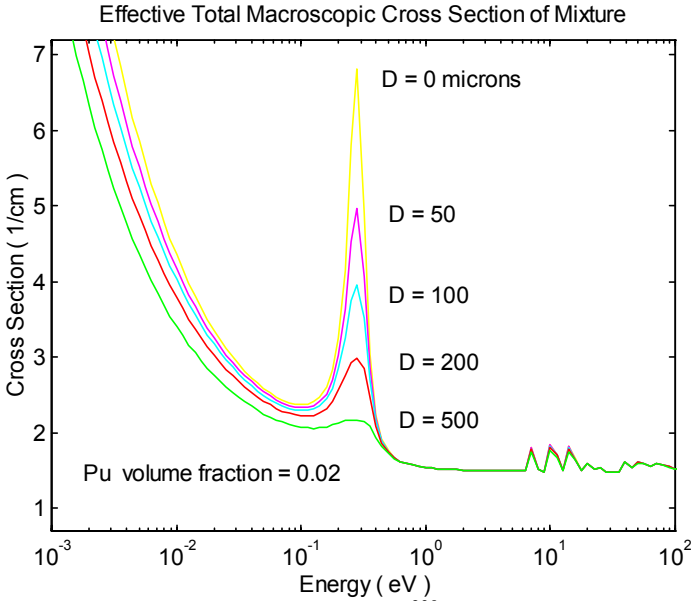

Figure 1. Effective Total Macroscopic Cross Sections of ^{239}Pu-Water Mixture for Spherical Pu Particles.

[1] This definition of J differs slightly from that given in [5]. However, the result is the same.

3. EFFECTIVE MICROSCOPIC CROSS SECTIONS OF MATRIX AND INCLUSION MATERIALS

Effective microscopic cross sections of matrix materials σ^i_m and inclusion materials σ^i_a can be calculated using expressions (15) and (16) with correction factors S_{hm} and S_{ha}, which depend on the particle shape and size.

$\sigma^i_m=\sigma^i S_{hm}$ for all materials of matrix (here H and O) (15)

$\sigma^i_a=\sigma^i S_{ha}$ for all materials of particle (here Pu) (16)

The σ^i 's are the usual microscopic cross sections of the material, or isotope. No other changes are necessary.

Note that if an element or isotope is present both in the matrix and in inclusions, it will have different nuclear constants after the cross sections are corrected. For example, consider a mixture of PuO_2 in H_2O. The Monte Carlo code must have the ability to include different variants of the same element (in this case oxygen). This is the only limitation for utilization of the effective cross section method.

Formulas for S_{hm} and S_{ha} for the case of **cubic particles** of edge h are

$$S_{hm} = \frac{\bar{\Sigma}/\Sigma_m}{\left(1-\alpha+\alpha\times\dfrac{1-\exp(-\Sigma_a h)}{1-\exp(-\Sigma_m h)}\right)}, \tag{17}$$

$$S_{ha} = \frac{\bar{\Sigma}/\Sigma_a}{\left(\alpha+(1-\alpha)\times\dfrac{1-\exp(-\Sigma_m h)}{1-\exp(-\Sigma_a h)}\right)}. \tag{18}$$

The effective total macroscopic cross section $\bar{\Sigma}$ for cubic particles (13) is used.

Recall that Σ_a is the total macroscopic cross section of particle material, Σ_m is the total macroscopic cross section of matrix material, $\Delta\Sigma = \Sigma_a - \Sigma_m$, and α is the volume fraction of particle material in the medium.

Formulas for S_{hm} and S_{ha} include the relative collision probabilities of neutrons in particle material and in matrix material. For cubic particles whose macroscopic cross section is (13), the probability of collision in particle material is proportional to $\alpha(1-\exp(-\Sigma_a h))$, and the probability of collision in matrix material is proportional to $(1-\alpha)(1-\exp(-\Sigma_m h))$.

Formulas for S_{hm} and S_{ha} for the case of **spherical particles** of diameter D are

$$S_{hm} = \frac{\bar{\Sigma}\left\{1 - \exp(-\Sigma_m D)\cdot\left(1 - q + qJ_{(-D\Delta\Sigma)}\right) + q\cdot\exp(-\Sigma_m D/2)\left(J_{(D\Sigma_m/2 - D\Sigma_a)} - J_{(D\Sigma_m/2)}\right)\right\}}{\Sigma_m(1-\alpha)\cdot\left(1 - \exp(-\Sigma_m D)\cdot\left[1 - q + qJ_{(-D\Delta\Sigma)}\right]\right)}, \quad (19)$$

$$S_{ha} = \frac{\bar{\Sigma}\left(q\cdot\exp(-\Sigma_m D/2)\right)\cdot\left(J_{(D\Sigma_m/2)} - J_{(D\Sigma_m/2 - D\Sigma_a)}\right)}{\Sigma_a\alpha\left(1 - \exp(-\Sigma_m D)\cdot\left[1 - q + qJ_{(-D\Delta\Sigma)}\right]\right)}, \quad (20)$$

where $\bar{\Sigma}$, q and $J_{(x)}$ are defined in (14).

Note that for $h \longrightarrow 0$ the expected limits of $\bar{\Sigma}$, S_{hm} and S_{ha} are obtained: $\bar{\Sigma} \rightarrow \Sigma_{hom} = \Sigma_m + \alpha\Delta\Sigma$, $S_{hm} \rightarrow 1$ and $S_{ha} \rightarrow 1$. Thus the microscopic effective cross sections σ^i_m and σ^i_a approach their natural values.

In Figures 2 and 3 are the effective microscopic fission cross sections of Pu^{239} for a mixture of plutonium particles in water. The cross sections in Figure 2 are given for different spherical particle sizes at a constant volume fraction of Pu. In Figure 3 the cross sections are given for different volume fractions at constant particle size.

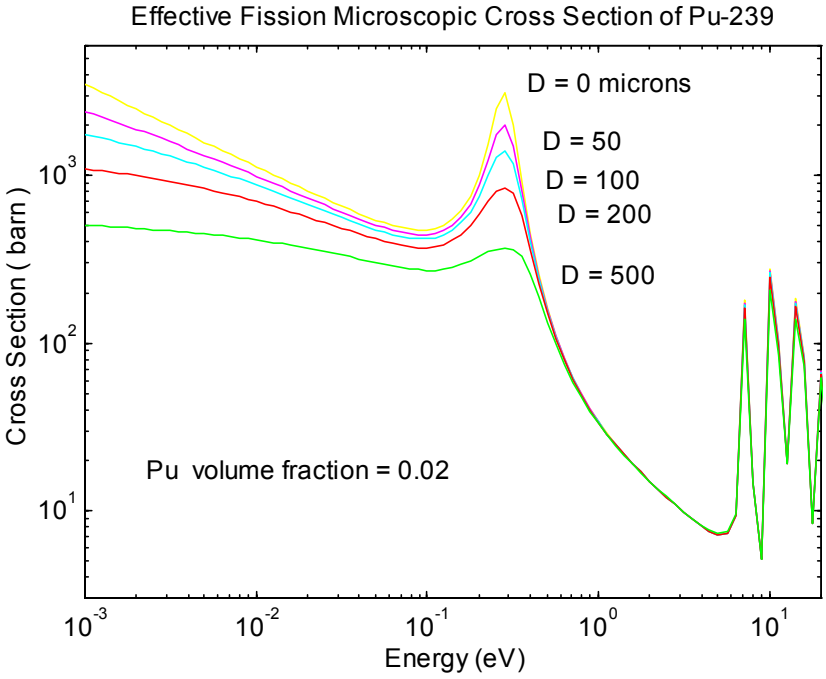

Figure 2. Effective Fission Cross Sections of ^{239}Pu in Water for Different Particle Diameters.

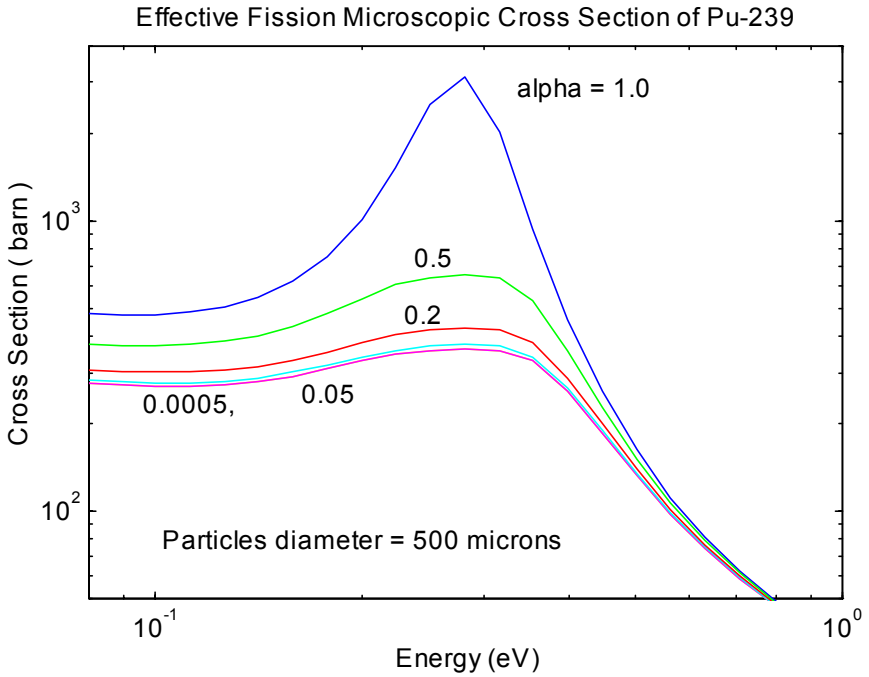

Figure 3. Effective Fission Cross Sections of ^{239}Pu in Water for Different Volume Fractions α.

For effective macroscopic total cross sections, it is easy to show that for $h_1<h_2$ the following relation is true:

$$\bar{\Sigma}(h_2) < \bar{\Sigma}(h_1) \le \Sigma_{hom} . \qquad (21)$$

The result is that neutron leakage from the system increases with increase of particle size. This is one reason why K_{eff} decreases as particle size increases. Note that relation (21) is true for any energy only for the effective macroscopic total cross sections of the mixture. For microscopic cross sections there is no such simple law. They can both increase and decrease.

4. ABOUT THE TRAJECTORY MODELING SCHEME IN DISPERSED MEDIA

As was mentioned above, the new, effective nuclear data of materials with inclusions consist of corrected reaction cross sections of all energies. However, there is no change in the energy and angular distribution of secondary particles formed in the specific reactions. The traditional trajectory modeling scheme is used with the effective cross sections.

Bringing in the factors S_{ha} and S_{hm} allows accounting for the probability of reactions being in particle material or in matrix material in the transport equation simply by modifying the cross sections. Purely speaking, it allows use of Monte Carlo codes without making any changes except to cross sections.

The direct, trajectory modeling scheme by the Monte Carlo method in dispersed media (calculation of K_{dir}) takes into account the probability of radiation entering an inclusion by discrete modeling of particles in the matrix. This is in contrast to our scheme of calculation with effective cross sections (calculation of K_{ehom}).

The main differences of this model (K_{ehom} calculation) from the traditional ones (either K_{dir} or K_{hom} calculations) are the following:

1. Use of an effective total cross section to determine the mean free path length in homogenized polydispersed medium.
2. Use of collision probability in the matrix and included particles that assumes random selection of sort of particle, k.

After these two steps, as in the traditional scheme, we can raffle reactions, number of secondary particles, their energies and outgoing angles, depending on the selection of particle type in step 2. Then, the steps are repeated for the next collision.

The cross sections are calculated using the formulas given above. The probability of collision with a k-type particle is q_k. Then the probability of collision of the considered radiation with matrix will be $1-\sum_k q_k$. At this time, this suggested scheme for more than one particle type has not been thoroughly tested with calculations and is only theoretical.

5. SUMMARY OF PREVIOUS CALCULATIONAL RESULTS

Before describing our recent calculations to find the limits of particle size for this method, we summarize our previous findings [4]. Our earlier investigations had two goals. The first goal was to determine quantitatively the particle size effect on the neutron-transport properties of the material. The second was to check the ability to successfully apply the new method of effective homogenization of cross sections.

In the report [4], criticality of large spherical systems consisting of a mixture of spherical ^{239}Pu fragments in a matrix of water was researched. The diameters of Pu fragments were from 5 μm to 500 μm for volume fractions of Pu in water from 0.0005 up to 0.5.

5.1 DETERMINING THE PARTICLE EFFECT WITH DIRECT CALCULATIONS

For the purpose of determining the effect of particle size of a fissile material in moderator, the system Pu+H_2O from [6] was chosen. That report gives the dependence of ^{239}Pu mass in the critical system of ^{239}Pu and water on ^{239}Pu partial density in water. These mixtures were taken as the starting homogeneous systems in order to determine the particle size effect. The following combinations of Pu volume fractions, α (or H/Pu), and ^{239}Pu particle diameter D were considered:

D, microns = [5 10 25 50 100 200 500]; (I_D=1,2,…7. Seven options in D, total)
α = [0.0005 0.001 0.002 0.005 0.02 0.05 0.2 0.5], that correspond to the following H/Pu ratios:
H/Pu = [2654.2 1326.4 662.6 264.2 65.1 25.2 5.3 1.3]; (J_α=1,2,…8. Eight options in α)

The radii of large spheres of Pu+H_2O mixture were chosen for each volume fraction in order to obtain K_{hom} close to 1 (using ENDF/B5).

Two types of K_{eff} were calculated using MCNP4a with ENDF/B5:

K_{dir} calculations were direct calculations of the heterogeneous system with a large number of the Pu particles distributed in the H_2O. Usual, unchanged neutron data were used.

K_{hom} values were calculated with the traditional homogenization of the system according to volume fractions, also without any change of the cross sections.

To set up the direct calculations, a cube of 125 cubic cells each with side s was used. In each of the cells one spherical particle from Pu was placed at random. Then an indefinite lattice was made from this cube

of 125 cells. From the obtained universe, a large sphere of required radius R was cut. The value s was calculated from the formula $\alpha s^3=\pi D^3/6$.

Tables I and II show different parameters of the system and results calculated with ENDF/B5.

Table I. System Parameters and Neutron Spectrum Initiating Fission in Homogeneous Water+^{239}Pu Media.

J_α	1	2	3	4	5	6	7	8
α	0.0005	0.001	0.002	0.005	0.02	0.05	0.2	0.5
R, cm	39.8	22	17.8	15.9	15.05	14.2	11.25	7.96
H/Pu → Energy, MeV ↓	2654	1326	663	264	65	25	5.3	1.3
0 - 10^{-6}	0.988	0.980	0.965	0.923	0.755	0.539	0.133	0.007
10^{-6} - 0.1	0.011	0.018	0.031	0.067	0.204	0.362	0.514	0.276
0.1 - 20	0.001	0.002	0.004	0.010	0.041	0.099	0.353	0.717

Table II. Direct Calculations, K_{dir} (σ, %) with ENDF/B5 for Spherical Water Systems with Inclusions of Spherical ^{239}Pu Particles.

D, μm	J_α	1	2	3	4	5	6	7	8
	$\alpha\rightarrow$	0.0005	0.001	0.002	0.005	0.02	0.05	0.2	0.5
	$I_D\downarrow$								
0*	0	1.003 (.15)	0.997 (.14)	0.998 (.11)	1.000 (.08)	1.000 (.10)	1.000 (.10)	1.000 (.10)	1.000 (.10)
5	1	0.997 (.2)	0.992 (.2)	0.996 (.15)	0.999 (.14)	0.999 (.15)	1.002 (.30)	1.001 (.30)	1.001 (.22)
10	2	0.994 (.14)	0.989 (.2)	0.994 (.2)	0.999 (.12)	0.999 (.13)	0.999 (.15)	0.999 (.16)	0.999 (.16)
25	3	0.981 (.15)	0.977 (.24)	0.991 (.17)	0.998 (.16)	0.998 (.16)	0.999 (.13)	0.999 (.13)	1.001 (.22)
50	4	0.957 (.2)	0.964 (.12)	0.980 (.3)	0.998 (.2)	0.998 (.2)	1.000 (.30)	0.998 (.16)	1.000 (.22)
100	5	0.910 (.17)	0.931 (.4)	0.966 (.3)	0.994 (.2)	0.998 (.24)	1.000 (.30)	0.996 (.26)	1.001 (.22)
200	6	0.826 (.2)	0.874 (.2)	0.931 (.26)	0.984 (.2)	1.004 (.14)	1.006 (.30)	1.000 (.28)	1.000 (.22)
500	7	0.646 (.3)	0.727 (.13)	0.827 (.3)	0.936 (.14)	1.010 (.11)	1.013 (.16)	1.000 (.23)	1.005 (.21)

* Homogeneous calculations. For D=0, $K_{hom} = K_{dir}$.

Figure 4 shows the ratio K_{dir}/K_{hom} as a function of diameter D of the ^{239}Pu inclusions for different Pu volume content α.

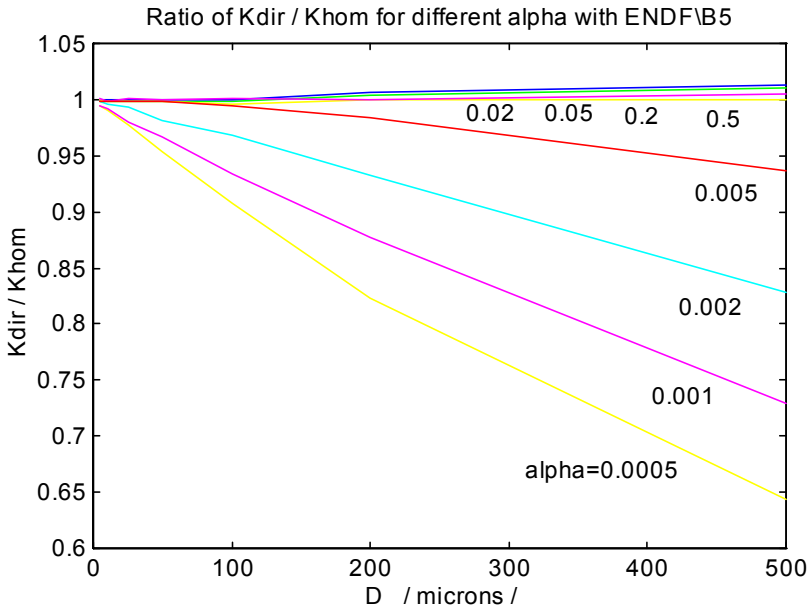

Figure 4. Ratio of K_{dir}/K_{hom} as a Function of ^{239}Pu Particle Diameter for Spherical Systems of Pu-Water Mixture.

As seen in Figure 4, even particle sizes as small as 50 microns have a significant effect on K_{eff} for low plutonium concentrations. Also notable is the slight upward trend of the ratio K_{dir}/K_{hom} as particle size increases for plutonium volume fractions larger than 0.01. This underprediction by K_{hom} of K_{eff} for larger particles can be seen more clearly in Figure 5, which shows the same curves as Figure 4 with the same horizontal axis but with vertical axis magnified. (Because of the relatively large standard deviations of the Monte Carlo calculations, these results are not conclusive.)

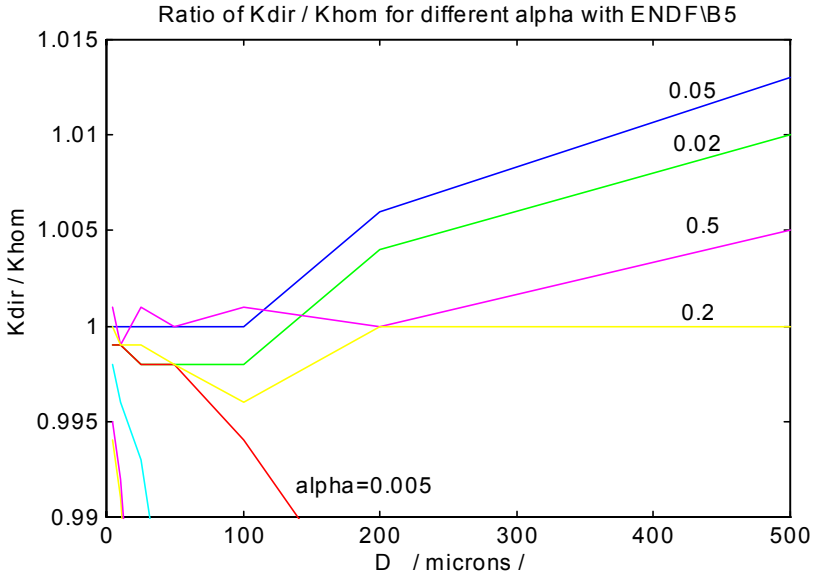

Figure 5. Same as Figure 4 with Magnified Vertical Axis.

5.2 CALCULATIONS WITH EFFECTIVE CROSS SECTIONS

Next, K_{dir}, K_{hom} and K_{ehom} were calculated in order to test the method of effective cross sections. For these calculations, in order to avoid some technical difficulties, we did not use ENDF/B5. Simplified (or model) cross sections were used in calculations of K_{hom}, K_{dir} and K_{ehom}. BAS-based simplified materials [7,8] were made for H, O and ^{239}Pu. The effective homogenized cross sections were also BAS-based. Use of BAS for development of the effective homogenized cross sections does not affect the principle of the method. Such an approach did not effect the results and speeded up our studies.

For calculations of K_{hom} and K_{dir} three simplified materials were made for H, O and ^{239}Pu. Their cross sections were indicated as ".01c" and recorded in the PUinW library. These materials were called the usual, or uncorrected materials. The following reactions (MT) were left in them: elastic and (n,γ) in H (2, 102); elastic in O (2); elastic, fission, inelastic 1, inelastic 2, inelastic to continuum, and (n,γ) in Pu (2, 18, 51, 52, 91, 102). All cross sections of these nine reactions were calculated at 222 common energy points. Other nuclear data for H, O, and Pu were also taken from BAS.

For the K_{ehom} calculations all cross sections of H, O and ^{239}Pu were recalculated. The effective cross sections for the matrix and inclusion materials were calculated from the formulas (15) and (16), where the correcting multipliers, S_{hm} (19) and S_{ha} (20), for the case of spherical particles were used. Materials for each combination "D,α", or "I,J", were made. They were indicated as ".IJc"; 3×7×8=168 of such materials were made (168+3) and recorded in the same PUinW library.

The parameters of the systems calculated using the PUinW library are given in Tables III through V. In these calculations the radii R of the large spheres are slightly different from the preceding ones for ENDF/B5 calculations. Note that the size of the system is constant for each value of α for both K_{dir} and K_{ehom} calculations of all particle sizes.

Table III. Parameters of the Systems (Large H_2O+Pu Spheres) Calculated with the PUinW Library.

J_α	1	2	3	4	5	6	7	8
α	0.0005	0.001	0.002	0.005	0.02	0.05	0.2	0.5
R, cm	40	22	18	16	15	14.25	11.3	8
M_{Pu} ,kg	2.68	0.89	0.98	1.72	5.65	12.12	24.18	21.50

Table IV. Direct Calculations of K_{dir} (σ, %) for the Large Spherical Systems of Water with Spherical ^{239}Pu Particles with the ".01c" Cross Sections from the PUinW Library.

D, μm	J_α / $\alpha\rightarrow$ / $I_D\downarrow$	1 0.0005	2 0.001	3 0.002	4 0.005	5 0.02	6 0.05	7 0.2	8 0.5
0*	0	.9826 (.10)	.9578 (.09)	.9777 (.08)	.9915 (.10)	.9924 (.07)	.9899 (.09)	.9740 (.06)	1.0018 (.06)
5	1	.9814 (.17)	.9582 (.28)	.9802 (.28)	.9957 (.27)	.9963 (.33)	.9910 (.28)	.9746 (.28)	0.9985 (.21)
10	2	.9782 (.15)	.9538 (.24)	.9715 (.30)	.9936 (.31)	.9968 (.29)	.9909 (.36)	.9755 (.28)	1.0003 (.20)
25	3	.9627 (.17)	.9382 (.22)	.9662 (.27)	.9856 (.29)	.9903 (.32)	.9884 (.29)	.9789 (.29)	1.0018 (.24)
50	4	.9445 (.19)	.9306 (.27)	.9568 (.26)	.9856 (.33)	.9846 (.32)	.9919 (.30)	.9712 (.28)	1.0007 (.24)
100	5	.8992 (.17)	.9005 (.23)	.9384 (.30)	.9769 (.33)	.9918 (.30)	.9836 (.36)	.9730 (.29)	1.0019 (.23)
200	6	.8333 (.20)	.8477 (.25)	.9079 (.27)	.9577 (.28)	.9942 (.31)	.9925 (.30)	.9727 (.28)	0.9979 (.23)
500	7	.6595 (.22)	.7088 (.25)	.8006 (.29)	.9125 (.33)	.9908 (.31)	.9942 (.29)	.9760 (.30)	1.0020 (.23)

* Homogeneous calculations. For D=0, $K_{hom} = K_{dir} = K_{ehom}$.

Table V. K_{ehom} (σ, %) Calculated for Homogeneous Spherical Systems of Water and ^{239}Pu with the ".IJc" Effective Cross Sections from the PUinW Library.

D, μm	J_α / $\alpha\rightarrow$ / $I_D\downarrow$	1 0.0005	2 0.001	3 0.002	4 0.005	5 0.02	6 0.05	7 0.2	8 0.5
0*	0	.9826 (.10)	.9578 (.09)	.9777 (.08)	.9915 (.10)	.9924 (.07)	.9899 (.09)	.9740 (.06)	1.0018 (.06)
5	1	.9810 (.14)	.9519 (.13)	.9742 (.13)	.9895 (.13)	.9921 (.12)	.9876 (.11)	.9737 (.11)	1.0028 (.18)
10	2	.9714 (.12)	.9515 (.14)	.9706 (.13)	.9890 (.13)	.9924 (.13)	.9876 (.11)	.9741 (.10)	1.0026 (.09)
25	3	.9643 (.14)	.9435 (.13)	.9642 (.14)	.9867 (.10)	.9907 (.10)	.9878 (.10)	.9730 (.08)	1.0038 (.09)
50	4	.9446 (.13)	.9276 (.13)	.9541 (.13)	.9860 (.12)	.9925 (.12)	.9868 (.12)	.9722 (.10)	1.0025 (.09)
100	5	.9019 (.12)	.9028 (.13)	.9376 (.14)	.9774 (.13)	.9930 (.13)	.9896 (.11)	.9744 (.10)	1.0006 (.09)
200	6	.8309 (.13)	.8459 (.14)	.9041 (.14)	.9603 (.13)	.9920 (.11)	.9901 (.09)	.9737 (.08)	1.0003 (.08)
500	7	.6681 (.12)	.7159 (.12)	.8061 (.15)	.9148 (.13)	.9898 (.14)	.9942 (.10)	.9747 (.10)	1.0045 (.16)

* Homogeneous calculations. For D=0, $K_{hom} = K_{dir} = K_{ehom}$

The results of the calculations with the PUinW library are plotted in Figure 6. The curves show the ratio K_{ehom}/K_{hom} as a function of diameter D of the ^{239}Pu inclusions for different Pu volume fractions, α. The ratios of K_{dir}/K_{hom} also shown as asterisks (*). The similarity to the curves of Figure 4, calculated with ENDF/B5 cross sections, indicate that the simplified cross section library preserves the essential cross-section effects. The coincidences of K_{dir}/K_{hom} data points with the K_{ehom}/K_{hom} curves indicate that the effective cross sections successfully represent the particle effects.

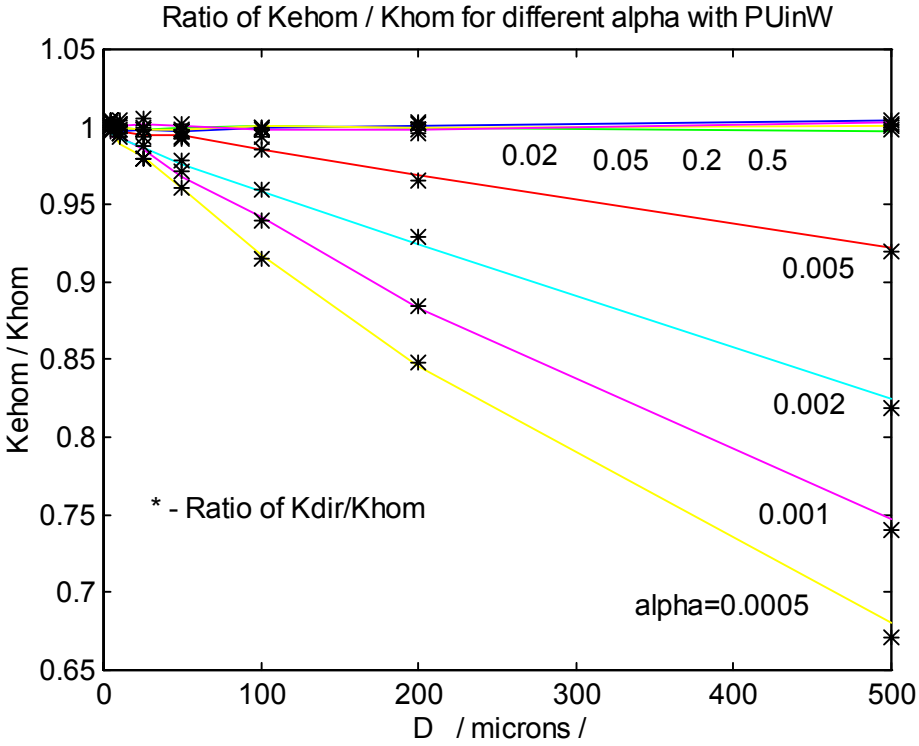

Figure 6. Ratio of K_{ehom}/K_{hom} as a Function of Particle Diameter for Different Pu Volume Fractions, α.

Table VI shows the difference between results of direct calculations with discrete particles, K_{dir}, and results of calculations using the effective cross sections, K_{ehom}. The differences are small, indicating good agreement between K_{dir} and K_{ehom}.

Table VI. Difference K_{ehom}-K_{dir} Obtained from Tables IV and V.

D, μm	J_α	1	2	3	4	5	6	7	8
	α→	0.0005	0.001	0.002	0.005	0.02	0.05	0.2	0.5
	I_D ↓								
5	1	-0.0004	-0.0063	-0.0060	-0.0062	-0.0042	-0.0034	-0.0009	0.0043
10	2	-0.0068	-0.0023	-0.0009	-0.0046	-0.0044	-0.0033	-0.0014	0.0023
25	3	0.0016	0.0053	-0.0020	0.0011	0.0004	-0.0006	-0.0059	0.0020
50	4	0.0001	-0.0030	-0.0027	0.0004	0.0079	-0.0051	0.0010	0.0018
100	5	0.0027	0.0023	-0.0008	0.0005	0.0012	0.0060	0.0014	-0.0013
200	6	-0.0024	-0.0018	-0.0038	0.0026	-0.0022	-0.0024	0.0010	0.0024
500	7	0.0086	0.0071	0.0055	0.0023	-0.0010	0	-0.0013	0.0025

The differences in Table VI are also shown in Figure 7. The apparent randomness of positive and negative differences can be attributed to the statistical nature of the Monte Carlo calculations.

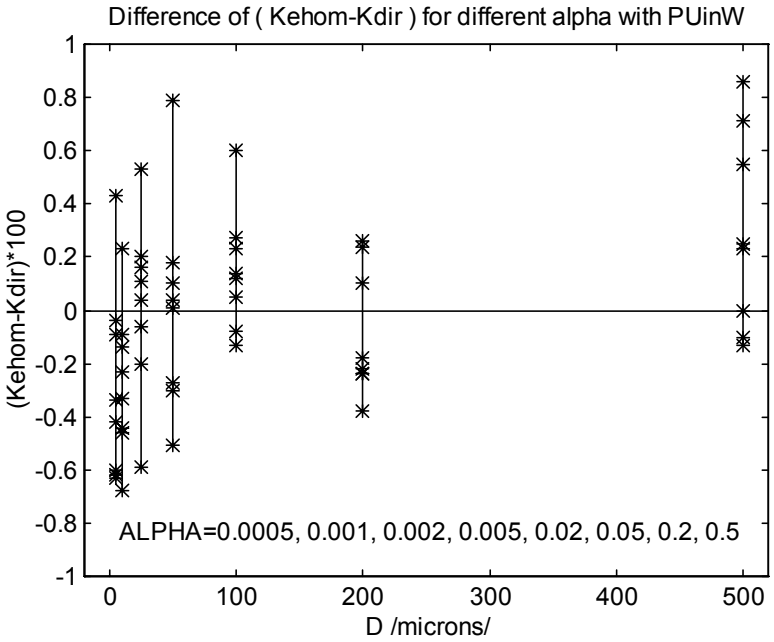

Figure 7. $K_{ehom} - K_{dir}$ for Different Pu Particle Diameters, D, and Volume Fractions, α.

5.3 SUMMARY OF PREVIOUS RESULTS

For all these combinations of volume fractions and sizes of fragments, no essential differences between K_{dir} and K_{ehom} were revealed, i.e. the differences between direct calculations of K_{dir} for an explicit representation of the heterogeneous medium and of K_{ehom} for a homogeneous medium with effective constants were small. That is, in our previous research, we did not manage to find out at what sizes of fragments the method of effective cross sections ceases to work.

6. CALCULATIONS WITH LARGER PARTICLES

6.1 DESCRIPTION OF CALCULATIONS

This latest work was directed to research of the question of where the effective cross sections fail for the Pu+Water system as particle size increases. For these calculations, the sizes of Pu fragments were ~100 times larger, from 0.1 cm up to 1 cm. The volume fractions of Pu in water varied from 0.0005 to 0.2, which correspond to H/Pu ratios from 2650 to 5.3. Rather than large spherical systems, large cubic blocks were used, so that there was no loss of Pu because of a cut of Pu fragments by an external surface of a system.

In the current task, the following combinations of Pu volume fractions, α (or H/Pu), and Pu particle diameter, D, were considered:

D, microns = [0.1 0.3 0.5 0.7 1.0] cm; (I_D=1,2,…5. Five options in D, total)

α = [0.0005 0.001 0.002 0.005 0.02 0.05 0.1 0.2], that correspond to the following H/Pu ratios:

H/Pu = [2650 1330 660 260 65 25 12 5.3]. (J_α=1,2,…8. Eight options in α)

The lengths of the sides of the large cubes of Pu+H_2O mixture were chosen for each volume fraction in order to obtain K_{eff} for the homogeneous case (D=0) close to 1.

Again, the same three types of K_{eff} were calculated:

K_{hom}, calculated with the traditional homogenization of the Pu+H_2O system.

K_{dir}, direct calculations of the heterogeneous system with a large number of Pu particles distributed in the H_2O.

K_{ehom}, calculations of the homogenized system with the effective cross sections of Pu, O and H.

For K_{hom} and K_{dir} calculations the simplified, or model, cross sections (".01c") for Pu, H and O were used. For K_{ehom} calculations we used the effective microscopic cross sections obtained from the model cross sections.

Because MCNP has a restriction on number of particles in one cell (< 1000), some calculations required the use of more than one cube for the system. If we found for the combination (D,α) that the number of particles was less than 1000 for a large cube the size of the entire system, we placed the particles randomly in all areas of the one large cube. Otherwise, we divided the side of the large cube an integer number of times to form smaller cubes, with each smaller cube requiring the same number of particles that was 1000 or less. Particles were placed randomly in all regions of the smaller cube. Then the entire system was built of the necessary number of smaller equivalent cubes.

In Figure 8 you can see part of one of the variants of the dispersed-medium model with n = 578 particles per smaller cube of side 5.331 cm, side of the cubic system = 31.986 cm, 6 small cubes per side, total number of particles = $n \times 6^3$ = 124848, D = 0.1 cm, α = 0.002.

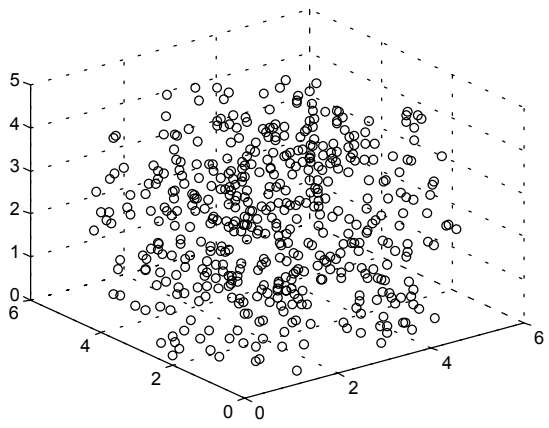

Figure 8. Model for a K_{dir} Calculation of 0.1-cm ^{239}Pu Particles in Water.

As in the previous calculations (Section 5.2), because of technical difficulties, we did not use ENDF/B5. Instead, BAS-based simplified materials were made for H, O and ^{239}Pu. The same reactions as in previous calculations were included. The new library of cross sections for mixtures with these larger particles was called PuW2000.

For K_{ehom} calculations all cross sections of H, O and ^{239}Pu were recalculated. Materials for each combination "D,α", or "I,J", were made. They are indicated as ".IJc"; $3 \times 5 \times 8 = 120$ of such materials were made (120+3) and recorded in the library PuW2000.

Effective microscopic cross sections of matrix materials σ^i_m and inclusion material σ^i_a were calculated using expressions (15) and (16) with correcting factors S_{hm} (19) and S_{ha} (20) for the case of spherical

particles. Plurality, energy and angle distributions of secondary particles were not corrected and remained in the reactions without any changes.

Figure 9 shows the variation of S_{ha} factors with neutron energy for Pu microscopic cross sections for spherical particles for all 40 combinations of D and α. A small area of Figure 9 for one volume fraction is shown in Figure 10. Figure 11 shows the S_{hm} factors for all 40 combinations of D and α for the microscopic cross sections of H and O. Figure 12 shows the S_{hm} factors for H and O for one particle diameter.

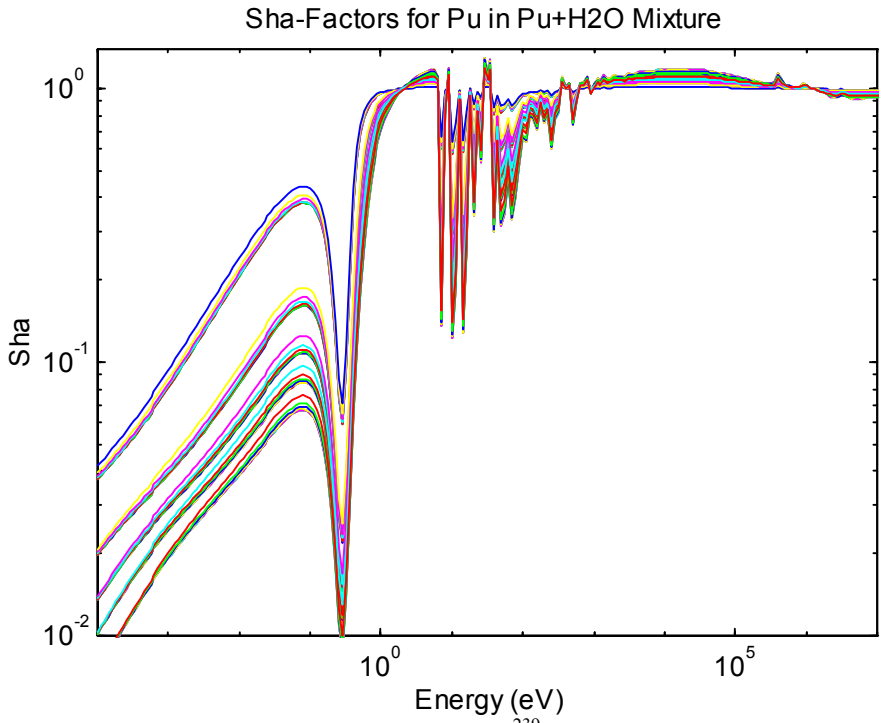

Figure 9. Variation of the Factor S_{ha} for ^{239}Pu Cross Sections with Energy for Spherical ^{239}Pu Particles for the Various Combinations of D and α.

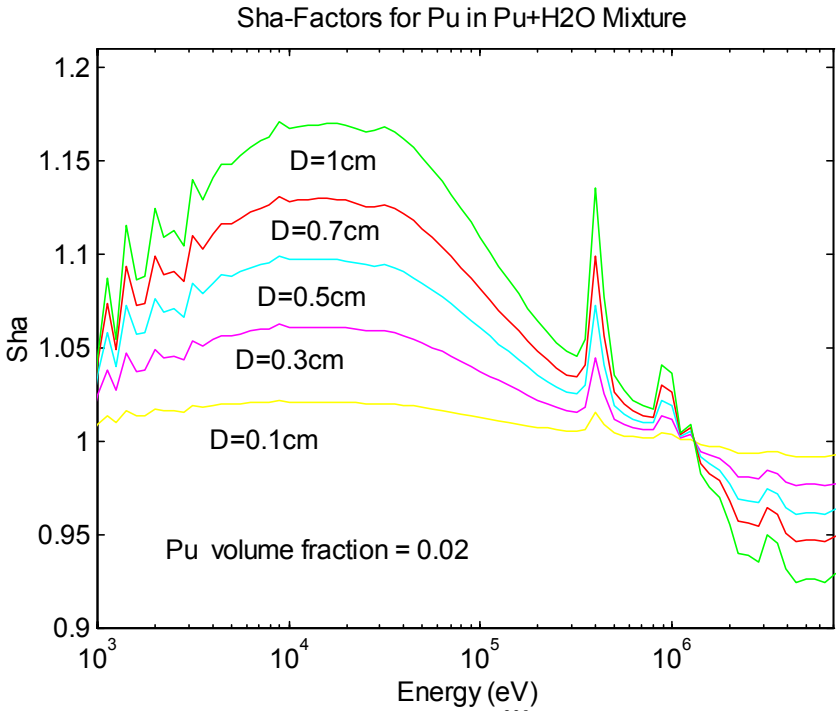

Figure 10. Variation of the Factor S_{ha} for ^{239}Pu Cross Sections with Energy for Spherical ^{239}Pu Particles for Different Diameters and $\alpha = 0.02$.

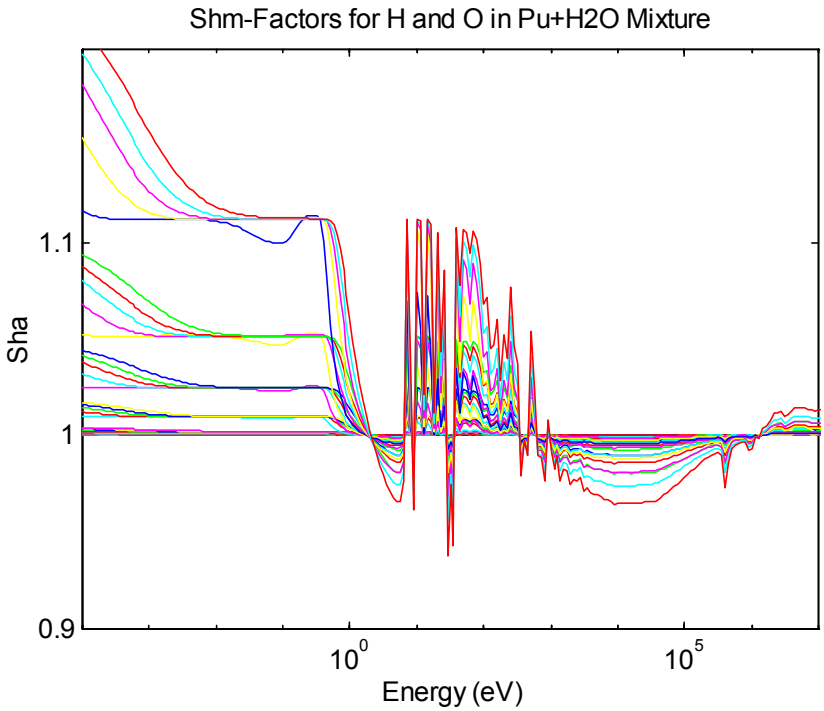

Figure 11. Variation of the Factor S_{hm} for H and O with Energy for Various Combinations of D and α.

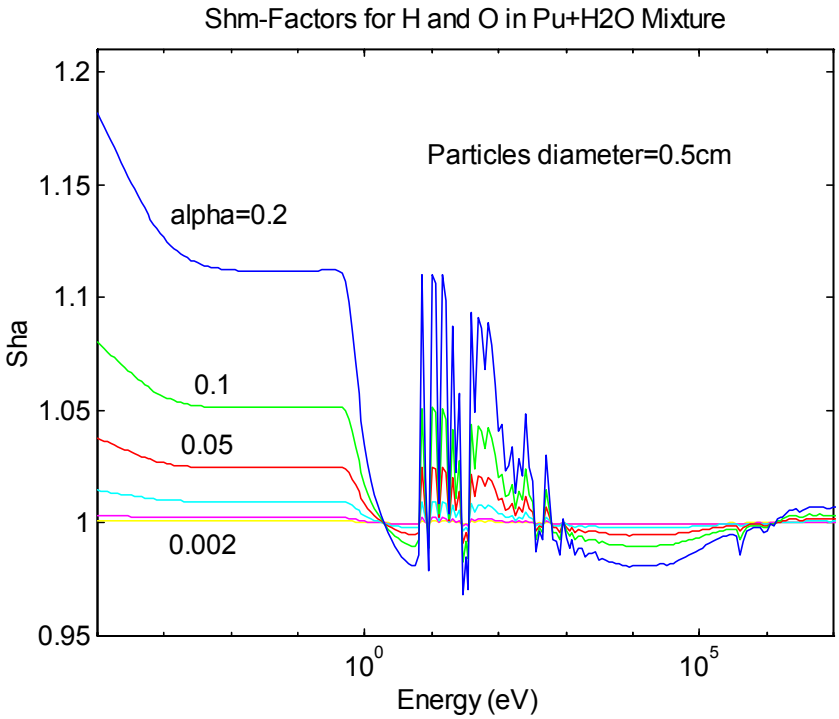

Figure 12. Variation of the Factor S_{hm} for H and O with Energy for ^{239}Pu Particle Diameter 0.5 cm.

6.2 RESULTS OF CALCULATIONS WITH LARGER PARTICLES

The parameters of the cubic systems calculated using the library PuW2000 are given in Tables VII through X. As in the previous calculations, the size of the system is constant for all particle sizes for each value of α. The parameter $Side_{crit}$ is the extrapolated value of the side of a critical cubic homogeneous solution system (D→0).

Table VII. Parameters of the Large Cubic Systems of H_2O+Pu Mixure for All Values of D.

α→ ↓	0.0005 J=1	0.001 J=2	0.002 J=3	0.005 J=4	0.02 J=5	0.05 J=6	0.1 J=7	0.2 J=8
$Side_{crit}$, cm	72.4	40.2	31.65	27.6	25.83	24.63	22.87	19.77
Side, cm	71.085	40.3	31.986	28.281	25.239	25.160	22.574	19.985
K_{hom}	0.9925	1.0013	1.0077	1.0208	0.9812	1.0180	0.9890	1.0090
M_{Pu} ,kg	3.587	1.307	1.307	2.257	6.424	15.904	22.991	31.918
H/Pu	2650	1330	660	260	65	25	12	5.3

Table VIII. Direct Calculations, K_{dir} (σ<0.1%), for the Large Cubic Systems of Water with Inclusions of Spherical ^{239}Pu Particles, with ".01c" Cross Sections from the PuW2000 Library.

D, cm	J_α / $\alpha\rightarrow$ / $I_D\downarrow$	1	2	3	4	5	6	7	8
	$\alpha\rightarrow$	0.0005	0.001	0.002	0.005	0.02	0.05	0.1	0.2
0*	0	0.9925	1.0013	1.0077	1.0208	0.9812	1.0180	0.9890	1.0090
0.1	1	0.4784	0.5713	0.6837	0.8511	0.9660	1.0277	0.9991	1.0124
0.3	2	0.2282	0.2954	0.3959	0.6002	0.8741	1.0123	1.0044	1.0239
0.5	3	0.1754	0.2272	0.3060	0.4669	0.7903	0.9832	1.0037	1.0303
0.7	4	0.1675	0.2103	0.2743	0.4231	0.7183	0.9532	0.9999	1.0365
1.0	5	0.1845	0.2119	0.2571	0.3651	0.6805	0.9064	0.9880	1.0424

* Homogeneous calculations. For D=0, $K_{hom} = K_{dir} = K_{ehom}$

Table IX. K_{ehom} (σ<0.1%) Calculated for the Large Cubic Systems of Homogenized Water and ^{239}Pu with the Effective ".IJc" Cross Sections from the PuW2000 Library.

D, cm	J_α / $\alpha\rightarrow$ / $I_D\downarrow$	1	2	3	4	5	6	7	8
	$\alpha\rightarrow$	0.0005	0.001	0.002	0.005	0.02	0.05	0.1	0.2
0*	0	0.9925	1.0013	1.0077	1.0208	0.9812	1.0180	0.9890	1.0090
0.1	1	0.4974	0.5901	0.7010	0.8618	0.9630	1.0230	0.9946	1.0093
0.3	2	0.2489	0.3242	0.4356	0.6457	0.8886	1.0104	0.9958	1.0134
0.5	3	0.1776	0.2384	0.3315	0.5362	0.8323	0.9923	0.9924	1.0131
0.7	4	0.1444	0.1965	0.2820	0.4723	0.7912	0.9767	0.9880	1.0146
1.0	5	0.1180	0.1626	0.2352	0.4124	0.7444	0.9551	0.9920	1.0118

* Homogeneous calculations. For D=0, $K_{hom} = K_{dir} = K_{ehom}$

Table X. Difference K_{ehom}-K_{dir} Obtained from Tables VIII and IX.

D, cm	J_α / $\alpha\rightarrow$ / $I_D\downarrow$	1	2	3	4	5	6	7	8
	$\alpha\rightarrow$	0.0005	0.001	0.002	0.005	0.02	0.05	0.1	0.2
0.1	1	0.0190	0.0188	0.0173	0.0107	-0.0030	-0.0047	-0.0045	-0.0031
0.3	2	0.0207	0.0288	0.0397	0.0455	0.0145	-0.0019	-0.0086	-0.0105
0.5	3	0.0022	0.0112	0.0255	0.0693	0.0420	0.0091	-0.0113	-0.0172
0.7	4	-0.0231	-0.0138	0.0077	0.0492	0.0729	0.0235	-0.0119	-0.0219
1.0	5	-0.0665	-0.0493	-0.0219	0.0473	0.0639	0.0487	0.0040	-0.0306

The results in the above tables are shown in Figures 13 and 14. The trends seen in Figure 6 continue in these figures as particle size increases. The K_{dir}/K_{hom} ratios, marked with asterisks (*), follow the curves for K_{ehom}/K_{hom}, as they did before for smaller particles. But the differences $K_{ehom} - K_{dir}$ are about an order of magnitude larger. (Particle diameters are ~2 orders of magnitude larger.)

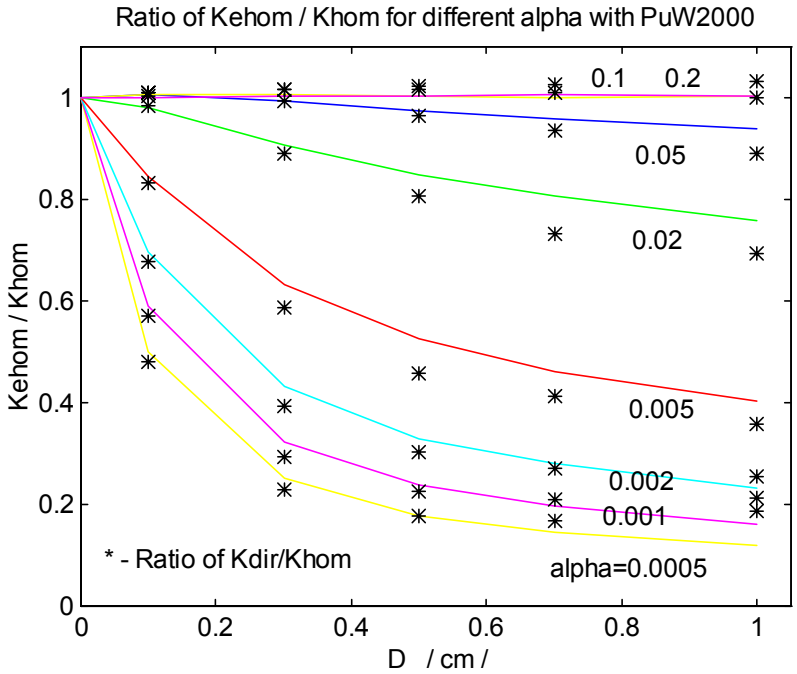

Figure 13. Ratio of K_{ehom}/K_{hom} (Curves) as a Function of Particle Diameter for Different Pu Volume Fractions, α, for Larger Particles.

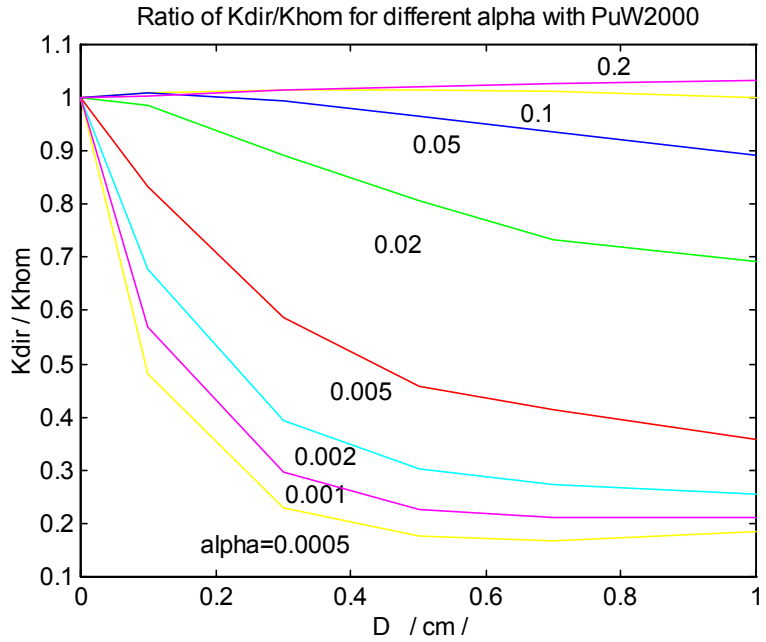

Figure 14. Ratio of K_{dir}/K_{hom} as a Function of Particle Diameter for Different Pu Volume Fractions, α, for Larger Particles.

Figure 14 is repeated in Figure 15 with the scale of the y-axis magnified to show the continuing upward trend of the ratio K_{dir}/K_{hom} with increasing particle size for large α, as was observed for smaller particles. Although it may be possible to explain the trend by spectral effects (due to a faster spectrum for larger α;

see Table I), it is impossible to predict without calculations whether similar trends will be observed for other plutonium systems, such as PuO_2+C or UO_2+PuO_2.

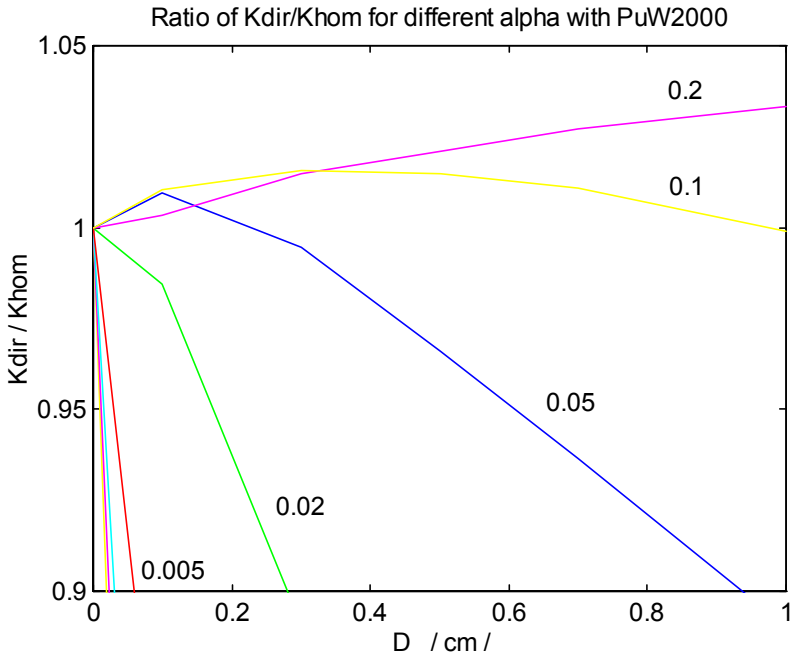

Figure 15. Same as Figure 14 with Magnified Vertical Axis.

The discrepancies between K_{ehom} and K_{dir} for larger particles can also be observed by considering their ratios, given in Table XI. These results are plotted in Figures 16 and 17. The largest discrepancies are for the lowest volume fractions of plutonium and for the largest particles. The agreement is fairly good for these large particles when the volume fraction is large. Small particles and small areas of matrix (right side of Figure 16 and left side of Figure 17, respectively) show good agreement of K_{dir} and K_{ehom} for the same reason (more spatial uniformity of flux).

Table XI. K_{ehom}/K_{dir} as Obtained from Tables VIII and IX.

D, cm	J_α	1	2	3	4	5	6	7	8
	$\alpha\rightarrow$	0.0005	0.001	0.002	0.005	0.02	0.05	0.1	0.2
	$I_D\downarrow$								
0.1	1	1.040	1.033	1.025	1.013	0.997	0.995	0.995	0.997
0.3	2	1.091	1.097	1.100	1.076	1.017	0.998	0.991	0.990
0.5	3	1.013	1.049	1.083	1.148	1.053	1.009	0.989	0.983
0.7	4	0.862	0.934	1.028	1.116	1.101	1.025	0.988	0.979
1.0	5	0.640	0.767	0.915	1.130	1.094	1.054	1.004	0.971

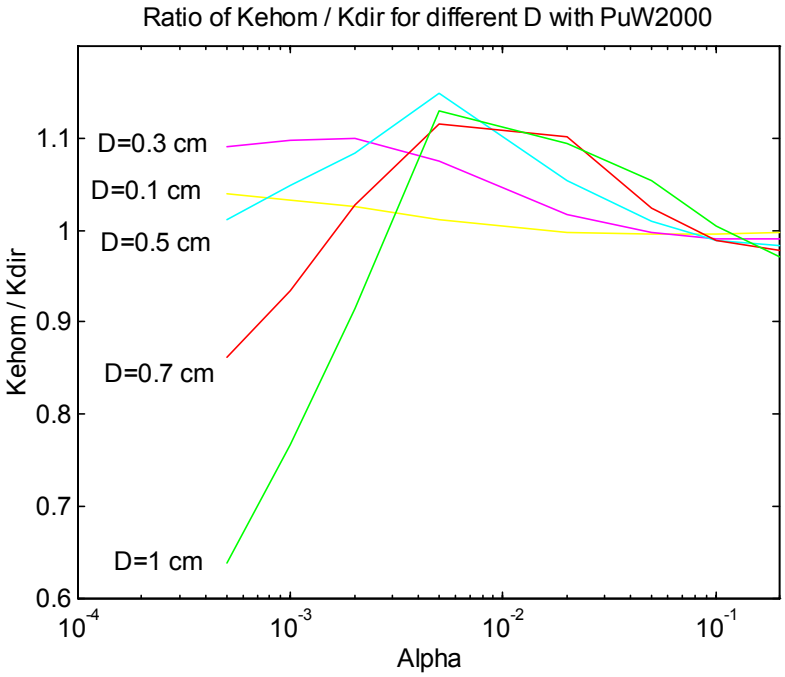

Figure 16. Ratio K_{ehom}/K_{dir} vs. Pu Volume Fraction α for Various Pu Particle Diameters.

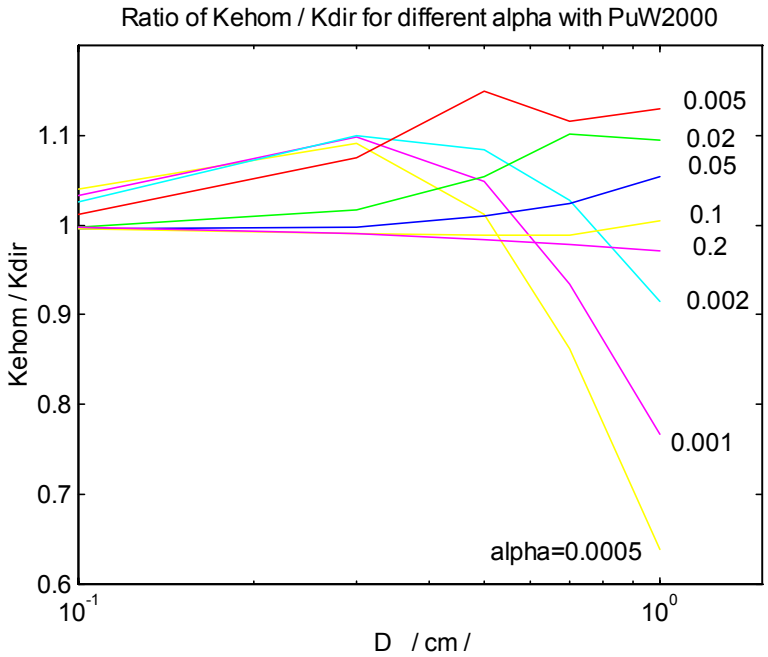

Figure 17. Ratio K_{ehom} / K_{dir} vs. Pu Particle Diameter for Various Pu Volume Fractions α.

7. CONCLUSIONS

Comparisons of results of criticality calculations with homogenized dispersed media using effective cross sections (K_{ehom}) with results of direct criticality calculations of particles dispersed in matrix (K_{dir}) indicate that the method of effective cross sections works. The formulas for effective cross sections successfully embody the effect of size of inclusions in a dispersed medium for a large range of particle sizes and inclusion volume fractions. The theory of the method is based on sound physical principals of attenuation of radiation in matter and collision probabilities of neutrons with matter, according to geometry of the particle-matrix mixture and nuclear cross sections of the particular materials.

Besides taking less time to run, calculations using the effective cross sections (K_{ehom}) are better than direct calculations (K_{dir}) in the sense that they use the average nuclear data for the dispersed media, rather than only one variant. A formula for dispersion of the flux, similar to equation (12), can be used to estimate the uncertainty of flux (and possibly estimate the additional uncertainty of K_{ehom}) from assuming average values (probabilities) due to random positions of particles.

Because of larger discrepancies between K_{ehom} and K_{dir} for the larger particle sizes (0.1–1 cm), limitations of the method have been found. However, the causes of the limitations are not yet clearly understood. So far, only one system (^{239}Pu particles in water) has been extensively calculated. Before the 'effective cross section method' is applied, further study is desirable.

The technique can be made more useful by future work on topics that extend the theory, better define its limits, and identify its applications. Possibilities are the following:

- Improve the formulas for spherical particles to extend the range of agreement with K_{dir} calculations.
- Test the method for systems with more than one particle type.
- Test the method for systems with absorber particles in fuel matrix.
- Apply the correction factors to other cross-section sets and test with other codes, including deterministic codes.
- Develop effective cross sections for various distributions of particle sizes.
- Provide formulas for calculating additional uncertainty of calculated K_{eff} due to assuming average random distribution of particles.
- Improve the correction factors S_{ha} and S_{hm} for non-spherical particles by integrating over all angles.
- Discover the parameters and formulas that define the limits of applicability.
- Develop particle size and shape specifications for advanced fuel mixtures.
- Calculate radiation resistance, dosimetry problems, problems of applied nuclear geophysics.
- Calculate the effect of particle size in composite materials used for shielding.
- Perform benchmark experiments with inclusions of well defined sizes and shapes to verify K_{dir} and K_{ehom} results.

ACKNOWLEDGMENTS

The authors express their sincere gratitude to Helen Cherepanova, Helen Lipilina, Gennadiy Orlov, Olga Verbitskaya and Vyatcheslav Sokolov for performing a large number of calculations, their help in processing neutron data files and creating the library PuW2000. They patiently repeated all this work every time when authors defined the formulas and code more exactly or found errors in the formulas and code. And this happened more than once.

REFERENCES

1. Newman, Darrell F., "Measurement of k_∞ and Relative Reaction Rates in an H_2O-Moderated UO_2-PuO_2 Particulate Fueled Lattice," *Nuclear Technology*, **Vol. 15**, August, 1972, pp. 192-208.

2. V.M.Shmakov. *"Effective cross sections of interaction photons with non-uniform absorbing media",* VANT. A series of a Technique and program of the numerical decision of mathematical physics problems, 1988, #1, pp.75-79 (in Russian)

3. V. M. Shmakov *"Effective Cross Sections of Radiation Attenuation and. Trajectory Modeling in Dispersed Media",* Thesis of the report to the VIII All Union Conference on the Monte Carlo Methods in Comp.Mathematics and Math.Physics, part 2, Novosibirsk, 1991, pp.123-126 (in Russian).

4. V.M. Shmakov, V.D. Lyutov, M.Yu. Smetanin, *"Model Calculations of Dispersed Media Criticality",* Proceedings of The Sixth International Conference on Nuclear Criticality Safety, ICNC'99, Versailles, France, Vol II, pp. 486-494, Sept 20-24, 1999.

5. V.M. Shmakov, *"Effective Cross Sections of Dispersed Media. Trajectory Modeling in Dispersed Media",* Proceedings of The Sixth International Conference on Nuclear Criticality Safety ICNC'99, Versailles, France, (CD-ROM), Sept 20-24, 1999.

6. Norman L. Pruvost, Hugh Paxton, "*Nuclear Criticality Safety Guide"*, p. 53, Figure 10, LA-12808, LANL, 1996.

7. A.P.Vasilyev, V.D. Lyutov, V.M.Shmakov, et al., *"Nuclear Data Library – BAS. The History of Development and Validation for Criticality Safety Calculations",* The Fifth International Conference on Nuclear Criticality Safety, ICNC'95, Versailles, France, V.1, p.2-59, 1995.

8. V.M.Shmakov, V.D.Lyutov, E.I.Cherepanova et al., "*Use of ENDF-format Libraries for Criticality Calculations at VNIITF",* The Sixth International Conference on Nuclear Criticality Safety, ICNC'99, Versailles, France, Vol. I, pp. 353-357, Sept 20-24, 1999.

9. J.Paratte, R. Chawla et al. *"Validation Efforts for Neutronics of an Employing PuO_2-Er_2O_3-ZrO_2 Inert Matrix Fuel"*, p.33, 4th Inert Matrix Fuel Workshop, October 19-20, 1998, PSI, Switzerland.